Stability Characterizations of Fixtured Rigid Bodies with Coulomb Friction*

J.S. Pang
Dept. of Math Sciences
Johns Hopkins University
Baltimore, Maryland 21218-2689, U.S.A.

J.C. Trinkle
Intellligent Systems Principle Dept.
Sandia National Labs
Albuquerque, NM 87185-1004, U.S.A.

Abstract. This paper formally introduces several stability characterizations of £xtured three-dimensional rigid bodies initially at rest and in unilateral contact with Coulomb friction. These characterizations, *weak stability* and *strong stability*, arise naturally from the dynamic model of the system, formulated as a complementarity problem. Using the tools of complementarity theory, these characterizations are studied in detail to understand their properties and to develop techniques to identify the stability classi£cations of general systems subjected to known external loads.

1 Introduction

Many useful mechanical systems are composed of a number of bodies that interact through multiple, unilateral frictional contacts. Examples include gears, cams, modular £xturing systems, and robot grippers. [1] Designers of such systems rely heavily on the analyses of initial designs, which are often carried out under the rigid body assumption. Nonetheless, signi£cant holes in both the relevant theory and computational tools remain. In this paper, we attempt to close one of those holes through a rigorous study of the stability of a free three-dimensional rigid body (called a workpiece) initially at rest and in frictional contact with £xed rigid bodies (called £xels). Our analysis is based on the theories of rigid body dynamics and complementarity. Our primary objective is to develop a sound basis that will enable us to gain a thorough understanding of the main issues involved with stability. Our secondary objective is to derive theoretical results that will enable the development of tests that more accurately characterize stability than the overly conservative tests in use today. The main results are presented in three new theorems and illustrated through a planar example.

*This research was partially supported by NSF grants CCR-9624018, IRI-9713034, and IRI-9619850, THECB grant ATP-036327-017, and Sandia, a multiprogram laboratory operated by Sandia Corporation, a Lockheed Martin Company, for the United States Department of Energy under contract DE-AC04-94AL85000.

[1] In fact at a £ne level of detail, every lower pair joint in every mechanism is actually implemented with a clearance, which leads to unilateral contacts in the joint interfaces.

1.1 Previous Work

There are two primary ways to stabilize a rigid workpiece. The £rst is known as form closure [5]. A workpiece is form-closed if it cannot move, even in£nitesimally, without at least one £xel penetrating the workpiece. This sort of stability does not rely on friction and is easy to check (by solving a linear program [11]). Several automated £xture design systems are based on form closure.[2] However, because form closure requires large numbers of contacts, it can sometimes be impossible to design form-closure £xtures that provide suf£cient access for machining tools or part insertions.

Recognizing the limitations of using large numbers of contacts, Palmer [8] and others have studied rigid body stability without form closure (*e.g.*, see [1, 4, 10, 14]). For such situations, the stability of the workpiece should be determined by examining the solution(s) to the dynamic model composed of the Newton-Euler equations for the workpiece, the relevant kinematic constraints, and appropriate friction laws. However, typically the dynamic equations are replaced by equilibrium equations, which can lead to false positive stability conclusions. In order to prevent this problem, the results in this paper are based on the dynamic equations.

Despite our beginning with a dynamic model, we do *not* adopt the usual stability de£nition for dynamic systems. The reason is that we allow sliding at the contacts which results in an irrecoverable loss of energy, and hence an arbitrarily perturbed workpiece will generally not return to its initial equilibrium con£guration. Instead, we will adopt Fourier's inequality [6]:

De£nition 1: If the acceleration of the workpiece is zero (for all solutions of the dynamic model) for given £xel locations and applied load, then the workpiece is said to be *stable*. Equivalently, a workpiece is stable if the virtual work for every kinematically admissible virtual motion is nonpositive. *Note that for convenience, we will also refer to the load and the £xture as being* stable *when this condition is met.*

Palmer found that determining stability (which he referred to as "in£nitesimal stability") in the presence of friction is ex-

[2] For an excellent review and extensive bibliography of many papers on this topic, see [2].

tremely dif£cult (co-NP complete), so he identi£ed two other stability classi£cations that could be tested ef£ciently by linear programming methods. These classi£cations were:

Potential Stability – Contact forces exists that satisfy equilibrium and Coulomb's law.

Guaranteed Stability – Contact forces exists that satisfy equilibrium without friction.

The primary problems with these stability characterizations are that they are overly conservative in one direction or the other, so their use in £xture design algorithms is limited. Figure 1 illustrates the problem. For a given £xture and workpiece con£guration, let SS($\boldsymbol{\mu}$) denote the set of *strongly stable* external loads (*i.e.*, those that satisfy stability De£nition 1 in the presence of friction, where $\boldsymbol{\mu}$ is the vector of friction coef£cients at the contact points). Similarly, let SS(0) denote the set of loads that are strongly stable without friction (Palmer's "guaranteed stability") and let WS($\boldsymbol{\mu}$) denote the set of *weakly stable* loads with friction (Palmer's "potential stability"). A load can be tested for membership in WS($\boldsymbol{\mu}$) or SS(0) using linear programming techniques, and as will be demonstrated, one can identify all the external loads in these sets for a given £xture. However, since there are loads in WS($\boldsymbol{\mu}$) that have multiple dynamic model solutions, some of which correspond to instability (nonzero workpiece acceleration), £xture design using this set is not recommended. On the other hand, the set of loads SS(0) is usually a small subset of SS($\boldsymbol{\mu}$), so its use in design is also limited.

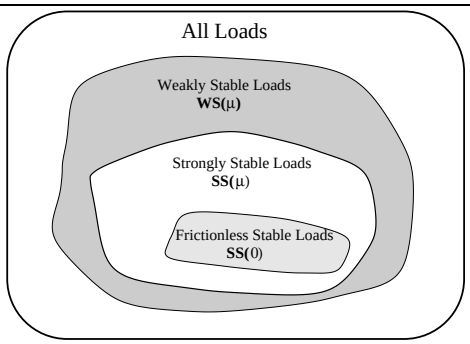

Figure 1: Important load subsets; SS$(0) \subseteq$ SS($\boldsymbol{\mu}$) $\subseteq$ WS($\boldsymbol{\mu}$).

Despite the limitations, Palmer's stability characterizations have been the best available for rigid £xture design without form closure. The results contained in this paper represent a signi£cant step toward stability tests which are not conservative, and hence could lead to better £xture design and analysis tools.

2 Methodology

Our basic framework is the discrete-time dynamic model for multiple rigid bodies in contact presented in [13]. By setting the initial velocity of the free body (the workpiece) to zero and £xing the positions of the actuated bodies (the £xels), this model represents a £xtured workpiece. Three sets of conditions are imposed on the workpiece: (a) the Newton-Euler equation written in terms of the contact accelerations, (b) conditions on the normal contact forces, and (c) Coulomb friction constraints on the tangential forces. These conditions, derived in [13], are listed below.

(a) The Newton-Euler equation:

$$\begin{bmatrix} \boldsymbol{a}_n \\ \boldsymbol{a}_t \\ \boldsymbol{a}_o \end{bmatrix} = \boldsymbol{A} \begin{bmatrix} \boldsymbol{c}_n \\ \boldsymbol{c}_t \\ \boldsymbol{c}_o \end{bmatrix} + \boldsymbol{b}, \tag{1}$$

where the subscripts n, t, o denote the normal (n) and two tangential directions (t, o) in the contact coordinate systems,

$$\boldsymbol{A} \equiv \mathcal{J}^T \mathcal{M}^{-1} \mathcal{J} \quad \text{and} \quad \boldsymbol{b} \equiv \mathcal{J}^T \mathcal{M}^{-1} \boldsymbol{g}_{\text{ext}}$$

with $\mathcal{J}$ being the system Jacobian matrix and $\mathcal{M}$ the system inertia matrix, the latter being symmetric positive definite, and $\boldsymbol{g}_{\text{ext}}$ being the external load applied to the workpiece. The vector $\boldsymbol{a}_n = (a_{in})_{i=1}^{n_c}$ is composed of the relative normal accelerations at the contacts indexed by i, where n_c is the number of contact points among the bodies. The relative accelerations in the tangential directions, t and o, are de£ned analogously. The vectors of normal wrench intensities, $\boldsymbol{c}_n$, and frictional wrench intensities, $\boldsymbol{c}_t$ and $\boldsymbol{c}_o$, are de£ned similarly. In the case of the £xture stability problem studied here, the system Jacobian matrix $\mathcal{J}$ is composed of wrench matrices $\boldsymbol{W}_n$ (in the normal direction), $\boldsymbol{W}_t$ and $\boldsymbol{W}_o$ (in the two tangential directions):

$$\mathcal{J} \equiv [\, \boldsymbol{W}_n \;\; \boldsymbol{W}_t \;\; \boldsymbol{W}_o \,].$$

These matrices simply map the contact forces into a common inertial coordinate frame. The matrix $\boldsymbol{A}$ can be written in partitioned form as follows:

$$\boldsymbol{A} = \begin{bmatrix} \boldsymbol{A}_{nn} & \boldsymbol{A}_{nt} & \boldsymbol{A}_{no} \\ \boldsymbol{A}_{tn} & \boldsymbol{A}_{tt} & \boldsymbol{A}_{to} \\ \boldsymbol{A}_{on} & \boldsymbol{A}_{ot} & \boldsymbol{A}_{oo} \end{bmatrix},$$

where for $\nu, \eta \in \{n, t, o\}$, $\boldsymbol{A}_{\nu\eta} \equiv \boldsymbol{W}_\nu^T \mathcal{M}^{-1} \boldsymbol{W}_\eta$. Similarly, the vector $\boldsymbol{b}$ can be written as: $\boldsymbol{b} = \begin{bmatrix} \boldsymbol{b}_n^T & \boldsymbol{b}_t^T & \boldsymbol{b}_o^T \end{bmatrix}^T$, where for $\eta \in \{n, t, o\}$, $\boldsymbol{b}_\eta \equiv \boldsymbol{W}_\eta^T \mathcal{M}^{-1} \boldsymbol{g}_{\text{ext}}$.

(b) Normal contact conditions:

$$0 \leq \boldsymbol{a}_n \perp \boldsymbol{c}_n \geq 0, \tag{2}$$

where the notation $\perp$ means perpendicularity. Note that this condition expresses the complementary relationship between the normal load and acceleration at each unilateral contact.

(c) Constraints on tangential forces: for $i = 1, ..., n_c$,

$$\begin{array}{rll} (c_{it}, c_{io}) \in & \text{argmin} & c'_{it} a_{it} + c'_{io} a_{io} \\ & \text{subject to} & (c'_{it}, c'_{io}) \in \mathcal{F}(\mu_i \, c_{in}), \end{array} \tag{3}$$

where $\mathcal{F}(\cdot)$ is the Coulomb friction map and μ_i is the nonnegative friction coef£cient at contact point i; that is, for each nonnegative scalar $\zeta \geq 0$, $\mathcal{F}(\zeta)$ is a planar circular disk with center at the origin and radius ζ:

$$\mathcal{F}(\zeta) \equiv \{\, (a,b) \in \Re^2 \,:\, a^2 + b^2 \leq \zeta^2 \,\}. \qquad (4)$$

Note that in the context of the quadratic Coulomb law (4), the "argmin" condition in (3) implies that the friction force opposes the direction of impending slip (we recall that the system is initially at rest).

The results developed in this paper apply to more general friction laws (including some axi-asymmetric laws (see [9])); nevertheless, for simplicity, we focus on the above standard Coulomb friction law.

Every set of contact forces $\boldsymbol{c} \equiv (\boldsymbol{c}_n, \boldsymbol{c}_t, \boldsymbol{c}_o)$ induces a vector of body accelerations $\ddot{\boldsymbol{q}}$, as follows:

$$\ddot{\boldsymbol{q}} \equiv \mathcal{M}^{-1}\,(\,\mathcal{J}\boldsymbol{c} + \boldsymbol{g}_{\text{ext}}\,). \qquad (5)$$

Letting $\boldsymbol{a} \equiv (\boldsymbol{a}_n, \boldsymbol{a}_t, \boldsymbol{a}_o)$ denote the vector of relative accelerations at the contacts and using the fact that the workpiece is initially at rest, we see that

$$\boldsymbol{a} \,=\, \mathcal{J}^T\,\ddot{\boldsymbol{q}}.$$

Based on the above model, we rede£ne our stability characterizations in terms of contact forces and we introduce terminology for the complementary characterizations for three-dimensional bodies with Coulomb friction laws:

De£nition 2: For a given external load $\boldsymbol{g}_{\text{ext}}$ and £xel and workpiece con£gurations, the workpiece (and £xture and load) is said to be:

Weakly Stable – if a set of contact forces exists that satis£es equations (1–3) and that induces zero body accelerations;

Strongly Stable – if every set of contact forces that satis£es equations (1–3) induces zero body accelerations;

Weakly Unstable (Palmer's in£nitesimal instability) – if it is not strongly stable;

Strongly Unstable (Palmer's guaranteed instability) – if it is not weakly stable.

2.1 Weak stability

Clearly, the load $\boldsymbol{g}_{\text{ext}}$ is weakly stable if and only if there exists a contact force vector $\boldsymbol{c}$ satisfying:

$$\begin{array}{c} \mathcal{J}\boldsymbol{c} + \boldsymbol{g}_{\text{ext}} \,=\, 0 \\ \boldsymbol{c} \,\in\, \boldsymbol{\mathcal{F}}(\boldsymbol{\mu}), \end{array} \qquad (6)$$

where $\boldsymbol{\mathcal{F}}(\boldsymbol{\mu})$ is the Coulomb friction cone; that is

$$\boldsymbol{\mathcal{F}}(\boldsymbol{\mu}) \equiv \prod_{i=1}^{n_c} \{\, (c_{in}, c_{it}, c_{io}) \,:\, c_{in} \,\geq\, 0,\, (c_{it}, c_{io}) \,\in\, \mathcal{F}(\mu_i c_{in}) \,\}$$

with $\boldsymbol{\mu} \equiv (\mu_i)$ is the vector of friction coef£cients μ_i at the contacts and $\prod$ represents the Cartesian product operation applied to the spaces of the contact forces.

Geometrically, the system (6) de£nes the cone of weakly stable loads:

$$\text{WS}(\boldsymbol{\mu}) \,\equiv\, \{\, \boldsymbol{g}_{\text{ext}} \,:\, \text{the system (6) is consistent} \,\}. \qquad (7)$$

This cone is the image of the friction cone $\mathcal{F}(\mu)$ under the linear transformation de£ned by the negative of the system Jacobian matrix $\mathcal{J}$; that is,

$$\text{WS}(\boldsymbol{\mu}) \,=\, -\mathcal{J}(\mathcal{F}(\boldsymbol{\mu})).$$

As will be seen, the cone $\text{WS}(\boldsymbol{\mu})$ will play a central role throughout our study. The complement of $\text{WS}(\boldsymbol{\mu})$ consists of the strongly unstable applied loads. We illustrate this cone in the example below.

Example: Consider a uniform laminar disk of mass m and radius R in the plane in contact with two immovable £xels and external loading $\boldsymbol{g}_{\text{ext}}$ as shown in Figure 2. The £xels are located by the angles θ_1 and θ_2 measured counterclockwise about the origin of an inertial coordinate frame $\{x, y\}$ centered in the disk. The normal contact forces, c_{1n} and c_{2n}, are directed from the £xels toward the center of the disk. The corresponding friction force components are tangent to the disk, with positive values of c_{it} assumed to produce clockwise (negative) moments. We wish to examine conditions on the angles $\theta_i \in (0, \pi)$ and the friction coef£cients μ_i so that an applied load $\boldsymbol{g}_{\text{ext}} \in \Re^3$ is weakly stable.

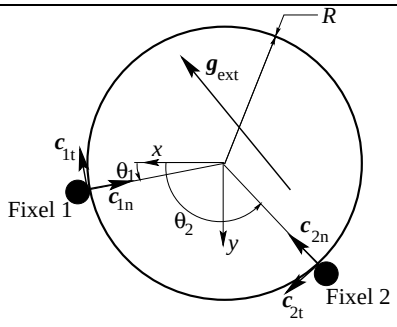

Figure 2: Loaded disk contacting two £xels.

The data for this problem are as follows. The problem is planar; thus there is only one tangential direction (no "o" direction) at each contact. There are two contact points; thus $n_c = 2$. Moreover we have:

$$\left[\; \boldsymbol{W}_n \;\middle|\; \boldsymbol{W}_t \;\right] \equiv \left[\begin{array}{cc|cc} -\cos\theta_1 & -\cos\theta_2 & \sin\theta_1 & \sin\theta_2 \\ -\sin\theta_1 & -\sin\theta_2 & -\cos\theta_1 & -\cos\theta_2 \\ 0 & 0 & -R & -R \end{array}\right]$$

$$\mathcal{M} \,=\, \left[\begin{array}{ccc} m & 0 & 0 \\ 0 & m & 0 \\ 0 & 0 & mR^2/2 \end{array}\right], \quad \boldsymbol{g}_{\text{ext}} \,=\, \left[\begin{array}{c} g_1 \\ g_2 \\ g_3 \end{array}\right].$$

Note that the analysis of this example is straight forward, but tedious, so is not included here. The interested reader can £nd the details in [9]. We restrict this presentation to the primary qualitative aspects.

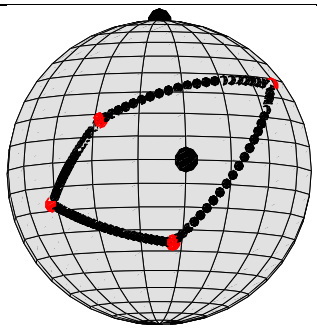

Figure 3: The set of weakly stable loads in $\Re^3$; $\mu_1 = 0.2$ and $\mu_2 = 0.5$.

The condition for the weak stability of $\boldsymbol{g}_{\text{ext}}$ is the existence of $\boldsymbol{c} = (c_{1n}, c_{2n}, c_{1t}, c_{2t})$ satisfying the following linear inequality system:

$$\mathcal{J}\boldsymbol{c} + \boldsymbol{g}_{\text{ext}} = 0 \quad (8)$$

$$|\, c_{it} \,| \leq \mu_i \, c_{in}, \quad i = 1, 2. \quad (9)$$

A contact force $\boldsymbol{c}$ satisfying equation (8) can be solved in terms of the friction force at the second contact c_{2t} and then substituted into the friction constraints to yield four inequalities linear in c_{2t}. These inequalities de£ne a convex cone of all weakly stable loads. Figure 3 shows WS($\boldsymbol{\mu}$) on the unit sphere centered at the origin of $\Re^3$ for $\mu_1 = 0.2$, $\mu_2 = 0.5$, $\theta_1 = \pi/4$, and $\theta_2 = 2.5\pi/4$. The generators of WS($\boldsymbol{\mu}$) are indicated by four medium-sized bubbles at the vertices of the "quadrilateral." Any external load passing through the interior or boundary of this "quadrilateral" has weak stability. Note that the g_3-direction (the moment direction) is indicated by the big bubble on the top of the sphere. The g_2-direction (the y-component direction of the external force) is marked by the big bubble inside the quadrilateral.

Figure 4 shows the two dimensional slice of WS($\boldsymbol{\mu}$) through the equator of the sphere shown in Figure 3, thus corresponding to $g_3 = 0$. In this case, the external loads in question are those representable as pure forces passing through the center of the disk. As expected, the set of weakly stable external forces are those contained in the convex cone formed by the radii to the contact points.

Further analysis of this example leads to two interesting cases summarized next.

Case 1. WS($\boldsymbol{\mu}$) = $\Re^3$

In this case, all loads are weakly stable and the situation is equivalent to "force-closure" as each friction cone contains the other contact point [7]. Force closure is obtained for this example, if and only if the smaller of the friction coef£cients is greater than 1.4966. In terms of the unit sphere in Figure 3, increasing the friction coef£cients corresponds to separating the generators (the vertices of the "quadrilateral"). Once the values of both friction coef£cients increase beyond 1.4966, the 4 generators positively span $\Re^3$.

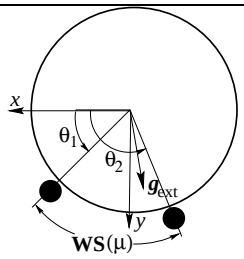

Figure 4: The set of weakly stable loads in $\Re^2$; $g_3 = 0$, $\mu_1 = 0.2$, and $\mu_2 = 0.5$.

Case 2. WS($\boldsymbol{\mu}$) degenerates into a "triangle."

In this case, the friction cone at one contact contains the other contact point, but the converse is not true. For this example, this situation arises when one friction coef£cient is greater than and the other is less than 1.4966. Figure 5 shows the set of weakly stable loads for $\mu_1 = 1.8$, $\mu_2 = 0.5$ with the other data remaining the same as above, $\theta_1 = \pi/4$ and $\theta_2 = 2.5\pi/4$. Again, the big bubble on the top of the sphere indicates the g_3-direction while the one on the equator represents the g_2-direction. Note that increasing μ_1 from 0.2 causes the two left-most generators in the "quadrilateral" shown in Figure 3 to separate following their great circle. When μ_1 reaches a value of 1.4966 the left-most generator from the original quadrilateral reaches the great circle de£ned by the two right-most generators, causing the "quadrilateral" to degenerate into a "triangle." Further increasing μ_1 to 1.8 yields the "triangular" set shown, with one of the original generators inside.

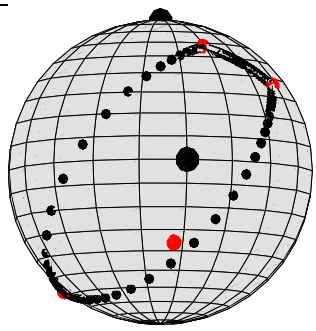

Figure 5: The set of weakly stable loads in $\Re^3$; $\mu_1 = 1.8$ and $\mu_2 = 0.5$.

Figure 6 shows the slice through the sphere corresponding to $g_3 = 0$. It is interesting to note that the set WS($\boldsymbol{\mu}$) has grown (by 0.08 radians) to include loads outside the cone formed by the radii to the contact points. □

We close this section by noting that it can be shown that decreasing any coef£cient of friction causes the set of weakly stable loads to contract monotonically:

$$\text{WS}(\boldsymbol{\mu}) \subseteq \text{WS}(\boldsymbol{\mu\prime}) \quad \text{if } \boldsymbol{\mu} \leq \boldsymbol{\mu\prime}.$$

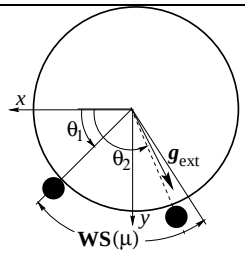

Figure 6: The set of weakly stable loads in $\Re^2$; $g_3 = 0$, $\mu_1 = 1.8$, and $\mu_2 = 0.5$.

3 Main Results

In this section, we present the main results pertaining to the stability concepts de£ned in the last section. We begin with a preliminary result that gives an equivalent way of describing strong stability. In essence, this result asserts that strong stability (*i.e.*, zero body accelerations, $\ddot{\boldsymbol{q}} = 0$) can be characterized as nonpositive virtual work (*i.e.*, $\ddot{\boldsymbol{q}}^T \boldsymbol{g}_{\text{ext}} \leq 0$); [3] this result is consistent with the asserted equivalence in Definition 1 of stability. A proof of the following proposition is given in appendix A in [9].

Proposition 1 *Let $\boldsymbol{g}_{\text{ext}}$ be a given applied load. The following statements are equivalent:*
(a) $\boldsymbol{g}_{\text{ext}}$ is strongly stable;
(b) every set of contact forces consistent with equations (1-3) yields nonpositive virtual work.
(c) $\boldsymbol{g}_{\text{ext}}$ is weakly stable and every set of equilibrium contact forces yields zero relative tangential accelerations, $\boldsymbol{a}_t$ and $\boldsymbol{a}_o$.

The distinction between weak stability and strong stability is clearly due to the nonuniqueness of the contact forces. If the dynamic rigid body contact model has a unique solution, then these two stability concepts are equivalent. Based on a uniqueness result obtained in [13], we state a suf£cient condition for this equivalence to hold. Subsequently, this result will be generalized.

Proposition 2 *Suppose that the Jacobian matrix $\mathcal{J}$ has full column rank. There exists a scalar $\bar{\mu} > 0$ such that if $\mu_i \in [0, \bar{\mu}]$ for all $i = 1, \ldots, n_c$, $\boldsymbol{g}_{\text{ext}}$ is weakly (un)stable if and only if it is strongly (un)stable.*

The scalar $\bar{\mu}$ has to do with the preservation of the "P-property" of certain perturbations of the matrix $\boldsymbol{A}$ (which is positive de£nite under the full rank assumption in the above proposition). For more discussion on this scalar, see [12].

[3] Note that since the system begins at rest, the instantaneous acceleration $\ddot{\boldsymbol{q}}$ is proportional to the instantaneous velocity $\dot{\boldsymbol{q}}$ and hence the expression given is proportional to the virtual work.

3.1 The role of frictionless stability

The frictionless problem corresponds to $\boldsymbol{\mu} = 0$. This case plays an important role in the frictional problem. For one thing, the frictionless case provides another instance where weak and strong stability are equivalent. This is part of the content of Theorem 1 below. Besides establishing the equivalence of weak and strong stability, this theorem also shows that frictionless stability is easy to check, namely, by solving a linear program. More importantly, frictionless stability is actually equivalent to (weak or strong) stability for all friction coef£cients. Thus we see that frictionless stability is a very desirable property. Note that while many have previously conjectured that frictionless stability implies strong stability with friction, we were not aware of a formal proof until now (see Appendix B of [9]).

Unlike Proposition 2, the theorem below and all subsequent results do not require $\mathcal{J}$ to have full column rank.

Theorem 1 *Let $\boldsymbol{g}_{\text{ext}}$ be a given applied load. The following £ve statements are equivalent:*
(a) There exists a vector $\hat{\boldsymbol{c}}_n$ satisfying

$$\boldsymbol{W}_n \hat{\boldsymbol{c}}_n + \boldsymbol{g}_{\text{ext}} = 0, \quad \hat{\boldsymbol{c}}_n \geq 0. \tag{10}$$

(b) The load $\boldsymbol{g}_{\text{ext}}$ is weakly stable for all $\boldsymbol{\mu}$.
(c) The load $\boldsymbol{g}_{\text{ext}}$ is strongly stable for all $\boldsymbol{\mu}$.
(d) The load $\boldsymbol{g}_{\text{ext}}$ is weakly stable when $\boldsymbol{\mu} = 0$.
(e) The load $\boldsymbol{g}_{\text{ext}}$ is strongly stable when $\boldsymbol{\mu} = 0$.

With the above result, it is natural to ask what happens if frictionless stability is absent. The next result asserts that if the workpiece possesses a certain "separation property", then frictionless instability implies strong instability in the case of small friction coef£cients; thus in this situation, there must be suf£cient friction at the contacts in order for strong, or even weak, stability to hold.

Theorem 2 *Suppose that there exists a vector $\boldsymbol{u}_n$ satisfying $\boldsymbol{W}_n^T \boldsymbol{u}_n > 0$. The following two statements are equivalent:*
(a) $\boldsymbol{g}_{\text{ext}}$ is unstable for the frictionless problem;
(b) there exists a scalar $\bar{\mu} > 0$ such that if $\mu_i \in [0, \bar{\mu}]$ for all $i = 1, \ldots, n_c$, $\boldsymbol{g}_{\text{ext}} \notin WS(\boldsymbol{\mu})$; that is, $\boldsymbol{g}_{\text{ext}}$ is strongly unstable for the problem with $\boldsymbol{\mu} \equiv (\mu_i)$.

The physical interpretation of the supposition of Theorem 2 (that is, the existence of the vector $\boldsymbol{u}_n$) is as follows. If there exists a generalized acceleration ($\boldsymbol{u}_n$) of the £xtured workpiece that would cause all contacts to separate simultaneously, then the external load is strongly unstable for all friction coef£cients suf£ciently small if and only if it is strongly unstable when there is no friction. Notice that the existence of such a separating acceleration $\boldsymbol{u}_n$ depends entirely on geometry and has nothing to do with the applied load. We say that the workpiece has the *separation property* if such an acceleration exists.

From Theorems 1 and 2, it becomes evident that the most difficult case for analyzing strong stability is when the load is not (strongly or weakly) stable in frictionless contact but becomes strongly stable when friction is present. A critical value of the friction coefficients where the transition from instability to (weak or strong) stability occurs (if it occurs at all) is unfortunately not known and is expected to be very difficult to determine in general. Nevertheless, such a value can be computed in special cases.

In order to illustrate Theorems 1 and 2, it will be useful to introduce the polyhedral cone defined by all nonnegative combinations of the columns of the matrix $-\boldsymbol{W}_n$; that is,

$$\mathrm{WS}(0) \equiv -\mathrm{pos}(\boldsymbol{W}_n) = \{\, \boldsymbol{g}_{\text{ext}} : \text{system (10) is consistent} \,\}.$$

Theorem 1 then says that this cone $\mathrm{WS}(0)$ is precisely the set of all applied loads $\boldsymbol{g}_{\text{ext}}$ that are strongly stable for all friction coefficients; moreover, Theorem 2 implies that if the workpiece has the separation property, then a load $\boldsymbol{g}_{\text{ext}} \notin \mathrm{WS}(0)$ is weakly (not necessarily strongly) stable only if there is sufficient friction at the contacts. We illustrate Theorems 1 and 2 further using the example from the last section.

Example (continued): Setting $\mu_1 = \mu_2 = 0$, we can show that the cone $\mathrm{WS}(0)$ consists of all loads (g_1, g_2, g_3) satisfying:

$$g_3 = 0 \tag{11}$$
$$g_1 \sin\theta_2 - g_2 \cos\theta_2 \geq 0 \tag{12}$$
$$-g_1 \sin\theta_1 + g_2 \cos\theta_1 \geq 0. \tag{13}$$

This closed cone consists of all pure forces passing through the center of the disk and passing between the two contacts or through one of them. It is the same set illustrated in Figure 4 as $\mathrm{WS}(\boldsymbol{\mu})$.

With $\boldsymbol{u}_n \equiv (0, -1, 0)$, we clearly have $\boldsymbol{W}_n^T \boldsymbol{u}_n > 0$. Thus the disk has the separation property. To illustrate Theorem 2, consider a load $\boldsymbol{g}_{\text{ext}} = (g_1, g_2, 0)$ that fails one of the two conditions (12) and (13), and therefore lies outside of $\mathrm{WS}(0)$. Such a load is illustrated in Figure 6. In order for this load to be weakly stable in the frictional case, the analysis in [9] implies that there must exist a scalar c_{2t} such that four certain inequalities, linear in c_{2t}, hold. From these inequalities, it is not difficult to verify that if

$$0 \leq \max(\,\mu_1, \mu_2\,) < \frac{sin(\theta_2 - \theta_1)}{1 - cos(\theta_2 - \theta_1)} = 1.4966 = \bar{\mu},$$

then there cannot exist any c_{2t} that balances $\boldsymbol{g}_{\text{ext}} \notin \mathrm{WS}(0)$. Theorem 2 is therefore verified. □

3.2 The WU_{R} sets

One of the primary goals of this paper is to identify the set of loads that are strongly stable (*i.e.*, members of $\mathrm{SS}(\boldsymbol{\mu})$) for a given friction coefficient. Since it is hard to identify such loads directly, we are interested in identifying loads that are weakly unstable ($\mathrm{WU}(\boldsymbol{\mu})$ and therefore known to lie outside $\mathrm{SS}(\boldsymbol{\mu})$). By Theorem 1, we know that loads lying outside of $\mathrm{SS}(\boldsymbol{\mu})$ must also lie outside the cone $\mathrm{SS}(0)$. In order to motivate the main result in this subsection, Theorem 3, we state a preliminary result pertaining to the frictionless problem. The next result is inspired by the concept of a complementary cone in linear complementarity theory [3].

Proposition 3 *If $\boldsymbol{W}_n$ has full row rank, an applied load $\boldsymbol{g}_{\text{ext}}$ is (weakly or strongly) unstable for the frictionless problem if and only if there exist a nonempty subset α of $\{1, \ldots, n_c\}$ with complement $\bar{\alpha}$ and nonnegative vectors $\boldsymbol{a}_{n\alpha}$ and $\boldsymbol{c}_{n\bar{\alpha}}$ with $\boldsymbol{a}_{n\alpha} \neq 0$ such that*

$$\boldsymbol{W}_n^T \mathcal{M}^{-1} \boldsymbol{g}_{\text{ext}} = \boldsymbol{I}_{\cdot\alpha} \boldsymbol{a}_{n\alpha} - (\boldsymbol{A}_{nn})_{\cdot\bar{\alpha}} \boldsymbol{c}_{n\bar{\alpha}}.$$

Here α and $\bar{\alpha}$ are the index sets of the contacts that are to be separated and maintained, respectively. The dot subscript following $\boldsymbol{A}_{nn}$ indicates that all rows of $\boldsymbol{A}_{nn}$ are included. Notice that Proposition 3 depends on the full row rank assumption of $\boldsymbol{W}_n$ to guarantee that if $\boldsymbol{a}_n = 0$, then $\ddot{\boldsymbol{q}} = 0$ also. Since this rank condition is rather restrictive, this requirement is removed in the next proposition. Without this restriction, the phrase "and only if" must be removed.

Proposition 4 *An applied load $\boldsymbol{g}_{\text{ext}}$ is (weakly or strongly) unstable for the frictionless problem if there exists a nonempty subset α of $\{1, \ldots, n_c\}$ with complement $\bar{\alpha}$ and nonnegative vectors $\boldsymbol{a}_{n\alpha}$ and $\boldsymbol{c}_{n\bar{\alpha}}$ with $\boldsymbol{a}_{n\alpha} \neq 0$ such that*

$$\boldsymbol{W}_n^T \mathcal{M}^{-1} \boldsymbol{g}_{\text{ext}} = \boldsymbol{I}_{\cdot\alpha} \boldsymbol{a}_{n\alpha} - (\boldsymbol{A}_{nn})_{\cdot\bar{\alpha}} \boldsymbol{c}_{n\bar{\alpha}}.$$

The equation in the above propositions can be easily derived from the original Newton Euler equation (1) by setting friction forces to zero and removing the equations corresponding to the tangential components of the contact accelerations.[4] Applying all subsets α of $\{1, \ldots, n_c\}$ to the equation represents all possible combinations of breaking and maintained contacts. We will henceforth refer to each such combination as a "contact mode." Note that the set of external loads corresponding to any particular contact mode is a convex cone. Thus we see that the set of applied loads, denoted $\mathrm{WU}_{\text{¤}}$, that are unstable for the frictionless problems can be described in terms of the union of finitely many polyhedra (the subscript "¤" denotes "frictionless").

Introducing friction into the problem, we define, for a given nonzero friction vector $\boldsymbol{\mu} \equiv (\mu_i)$, the set $\mathrm{WU}_{\mathrm{R}}(\boldsymbol{\mu})$ (the subscript "R" denotes "rolling"). consisting of all load vectors $\boldsymbol{g}_{\text{ext}}$ for which there exist a nonempty subset α of $\{1, \ldots, n_c\}$ with complement $\bar{\alpha}$, nonnegative vectors $\boldsymbol{a}_{n\alpha}$ and $\boldsymbol{c}_{n\bar{\alpha}}$ with $\boldsymbol{a}_{n\alpha} \neq 0$, and (free) vectors $\boldsymbol{c}_{t\bar{\alpha}}$ and $\boldsymbol{c}_{o\bar{\alpha}}$ such

[4] Note that the "and only if" could be reinserted into Proposition 4 if one adds enough additional linearly independent equations corresponding to nonzero values of the relative translational and relative angular accelerations at the contacts. However, we restrict our attention here to the present propositions.

that

$$\begin{aligned}
\boldsymbol{W}_n^T\mathcal{M}^{-1}\boldsymbol{g}_{\text{ext}} &= \boldsymbol{I}_{\cdot\alpha}\boldsymbol{a}_{n\alpha} \\
&\quad -(\boldsymbol{A}_{nn})_{\cdot\bar{\alpha}}\boldsymbol{c}_{n\bar{\alpha}} - (\boldsymbol{A}_{nt})_{\cdot\bar{\alpha}}\boldsymbol{c}_{t\bar{\alpha}} - (\boldsymbol{A}_{no})_{\cdot\bar{\alpha}}\boldsymbol{c}_{o\bar{\alpha}} \\
(\boldsymbol{W}_t^T\mathcal{M}^{-1}\boldsymbol{g}_{\text{ext}})_{\bar{\alpha}} &= \\
&\quad -(\boldsymbol{A}_{tn})_{\cdot\bar{\alpha}}\boldsymbol{c}_{n\bar{\alpha}} - (\boldsymbol{A}_{tt})_{\cdot\bar{\alpha}}\boldsymbol{c}_{t\bar{\alpha}} - (\boldsymbol{A}_{to})_{\cdot\bar{\alpha}}\boldsymbol{c}_{o\bar{\alpha}} \\
(\boldsymbol{W}_o^T\mathcal{M}^{-1}\boldsymbol{g}_{\text{ext}})_{\bar{\alpha}} &= \\
&\quad -(\boldsymbol{A}_{on})_{\cdot\bar{\alpha}}\boldsymbol{c}_{n\bar{\alpha}} - (\boldsymbol{A}_{ot})_{\cdot\bar{\alpha}}\boldsymbol{c}_{t\bar{\alpha}} - (\boldsymbol{A}_{oo})_{\cdot\bar{\alpha}}\boldsymbol{c}_{o\bar{\alpha}}
\end{aligned}$$

and

$$(\, c_{it}, c_{io}\,) \in \mathcal{F}(\mu_i c_{in}), \quad \forall\, i \in \bar{\alpha}.$$

These equations de£ne the set of external loads for which all contacts either separate or roll. Sliding is not allowed, as indicated by the absence of $\boldsymbol{a}_{t\alpha}$ and $\boldsymbol{a}_{o\alpha}$.

Of particular interest among these $\text{WU}_{\text{R}}(\boldsymbol{\mu})$ sets is $\text{WU}_{\text{R}}(0)$; this is clearly a subset of $\text{WU}_{\square}$; moreover, because the set $\text{WU}_{\text{R}}(\boldsymbol{\mu})$ does not include external loads corresponding to sliding contacts, we have

$$\text{WU}_{\text{R}}(\boldsymbol{\mu}) \subseteq \text{WU}_{\text{R}}(\boldsymbol{\mu}') \quad \text{if } \boldsymbol{\mu} \leq \boldsymbol{\mu}'. \tag{14}$$

In words, as the friction coef£cient increases, the set of weakly unstable loads with no sliding contacts grows.

The role of the WU_{R} sets is formally established in the result below.

Theorem 3 *If $\boldsymbol{g}_{\text{ext}} \in \text{WU}_{\text{R}}(\hat{\boldsymbol{\mu}})$ for some friction vectors $\hat{\boldsymbol{\mu}}$, then $\boldsymbol{g}_{\text{ext}}$ is weakly unstable for all friction vectors $\boldsymbol{\mu} \geq \hat{\boldsymbol{\mu}}$. In particular, if $\boldsymbol{g}_{\text{ext}}$ lies in $\text{WU}_{\text{R}}(0)$, then $\boldsymbol{g}_{\text{ext}}$ is weakly unstable (via a non sliding contact mode) for all friction coef£cients.*

Example (continued). For convenience, we take the disk radius $R = \sqrt{2}$ and the mass $m = 1$; thus $\mathcal{M}$ becomes the identity matrix. Further, de£ne the quantities: $r = \sin(\theta_2 - \theta_1)$ and $s = \cos(\theta_2 - \theta_1)$. Then, we have

$$\boldsymbol{A} = \left[\begin{array}{cc|c|c} 1 & s & 0 & -r \\ s & 1 & r & 0 \\ \hline 0 & r & 3 & 2+s \\ \hline -r & 0 & 2+s & 3 \end{array}\right].$$

Omitting the algebraic manipulations, we can obtain a complete description of the set $\text{WU}_{\text{R}}(\boldsymbol{\mu})$ as three convex cones. For this purpose, we de£ne several vectors:

$$g^1 \equiv \begin{bmatrix} -\sin\theta_1 \\ \cos\theta_1 \\ 0 \end{bmatrix}, \quad g^2 \equiv \begin{bmatrix} \sin\theta_2 \\ -\cos\theta_2 \\ 0 \end{bmatrix}$$

$$g^3 \equiv \begin{bmatrix} \sin\theta_1 \\ -\cos\theta_1 \\ 1/\sqrt{2} \end{bmatrix} \quad g^4 \equiv \begin{bmatrix} -\sin\theta_2 \\ \cos\theta_2 \\ -1/\sqrt{2} \end{bmatrix}$$

$$g^5 \equiv \begin{bmatrix} -\sin\theta_1 \\ \cos\theta_1 \\ \sqrt{2} \end{bmatrix} \quad g^6 \equiv \begin{bmatrix} -\sin\theta_2 \\ \cos\theta_2 \\ \sqrt{2} \end{bmatrix}$$

and $u^3 = (0, 0, 1)^T$. We have

$$\text{WU}_{\text{R}}(\boldsymbol{\mu}) = \text{WU}_{\text{R}_1}(\boldsymbol{\mu}) \cup \text{WU}_{\text{R}_2}(\boldsymbol{\mu}) \cup \text{WU}_{\text{R}_{12}},$$

where

$$\begin{aligned}
\text{WU}_{\text{R}_1}(\boldsymbol{\mu}) \equiv \{\, \boldsymbol{g}_{\text{ext}} \in \Re^3 \,|\, \boldsymbol{g}_{\text{ext}} &= x_1 g^3 + x_2(s g^1 + g^2) + x_3 g^5 \\
&\text{for some } (x_1, x_2, x_3) \ni x_1 > 0,\ |x_3| \leq \mu_1 x_2\}
\end{aligned}$$

$$\begin{aligned}
\text{WU}_{\text{R}_2}(\boldsymbol{\mu}) \equiv \{\, \boldsymbol{g}_{\text{ext}} \in \Re^3 \,|\, \boldsymbol{g}_{\text{ext}} &= x_1 g^4 + x_2(g^1 + s g^2) + x_3 g^6 \\
&\text{for some } (x_1, x_2, x_3) \ni x_1 > 0,\ |x_3| \leq \mu_2 x_2\}
\end{aligned}$$

$$\begin{aligned}
\text{WU}_{\text{R}_{12}} \equiv \{\, \boldsymbol{g}_{\text{ext}} \in \Re^3 \,|\, \boldsymbol{g}_{\text{ext}} &= -x_1 g^1 - x_2 g^2 + x_3 u^3 \\
&\text{for some } (x_1, x_2, x_3) \ni 0 \neq (x_1, x_2) \geq 0\}.
\end{aligned}$$

These sets are illustrated on the unit sphere in $\Re^3$ in Figure 7 for $\mu_1 = 0.2$ and $\mu_2 = 0.5$. The big bubble at the north pole is the positive g_3 axis, while the big bubble at the lower right points in the y-direction. The 5/16 sector of the sphere toward the back left corresponds to $\text{WU}_{\text{R}_{12}}$ and is independent of the values of the friction coef£cients. It becomes narrower as the contact points separate on the disk. The "triangular" set in the front delineates the loads in WU_{R_1}. The short leg of the triangle widens along its present great circle as μ_1 increases, as predicted by Theorem 3. As expected from the symmetry of this example, there is also a triangular set emanating from the other side of $\text{WU}_{\text{R}_{12}}$ with a leg that extends with increasing values of μ_2. The leg dependent on μ_2 is indicated by the small gray bubbles on the right horizon. It is interesting to note that the quadrilateral formed by the convex combination of the two extensible legs of the triangular regions is exactly the set $\text{WS}(\boldsymbol{\mu})$ shown in Figure 3 (as long as both friction coef£cients are less than 1.4966). The remaining uncharted regions on the sphere correspond to external loads which induce contact modes with at least one sliding contact as long as both friction coef£cients are less than 1.4966. Otherwise, some loads correspond to more than one contact mode. □

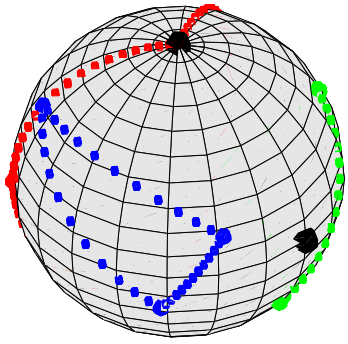

Figure 7: The set of weakly unstable loads in $\Re^3$; $\mu_1 = 0.2$ and $\mu_2 = 0.5$.

4 Conclusion

Motivated by the problem of £xture synthesis, we have studied the stability of a moveable rigid body (a workpiece) in frictional contact with several £xed rigid bodies (£xels). We have introduced the terms *weak stability* and *strong stability*

to characterize two types of "stability" of a £xtured workpiece. These classi£cations are particularly relevant to the situation in which the contact forces of the workpiece cannot be uniquely determined from Newton's Laws, the relevant kinematic constraints, and a friction law. Strong stability exists (for a given external load) when all admissible contact forces imply zero workpiece acceleration. This is the most desirable type of stability, because it provides absolute assurance that the workpiece will remain in place despite unknown internal stresses, however, strong stability is dif£cult to test.

The primary contribution of this paper is new insight into the stability problem derived from three theorems (a fourth theorem for the case of a linearized friction cone is derived in [9]) that provide ways to test for strong stability. While we have focused on the case of one workpiece, the extension to multiple workpieces is trivial. Speci£cally, the dimensions of the vectors and matrices appearing in the various equations increase, but the results and conclusions still hold. The three theorems are summarized below and illustrated in Figure 8 in the context of a disk in the plane in contact with two £xels. For simplicity, the £gure only applies to external loads which are pure forces passing through the center of the disk.

Theorem 1 presents (for the £rst time known to the authors) a formal proof that if a workpiece is (weakly or strongly) stable without friction, then it is strongly stable for all (positive) values of the friction coef£cients. For the example summarized in Figure 8, the external forces in the convex cone labeled "Theorem 1" are stable without friction. Theorem 1 implies that this cone is a subset of the set of all strongly stable loads for any (nonnegative) friction coef£cients.

Theorem 2 implies that weak and strong instability are equivalent when the friction coef£cients are below some bound. In general, this bound is dif£cult to £nd, but in some special cases, it can be computed easily. Returning to Figure 8, all external forces lying strictly outside the cone identi£ed by Theorem 1 are strongly and weakly unstable as long as both friction coef£cients are less than 1.4966.

Theorem 3 indicates that if for some external loading and friction coef£cients, the workpiece has a solution with a nonzero acceleration with all contacts rolling or breaking, then the workpiece is guaranteed to have a solution with the same contact mode if the friction coef£cients are increased. Figure 8 shows external loads corresponding to Theorem 3 as two convex cones bounding the Theorem 1 cone. The cones as drawn correspond approximately to friction coef£cients, $\mu_1 = 0.5$ and $\mu_2 = 0.8$ With no friction, the cones degenerate to the edges of the cone of Theorem 1. As the friction coef£cients go to in£nity, the edges of the cones move monotonically to the dashed lines (these are the edges of the normal cone of the SS(0)).

The results presented here leave several open questions for future study. Perhaps the most important questions relate to the computation of the friction bound appearing in Theorem 2 and the use of all the results in this paper in an effective £xture design and analysis system. We intend to address these questions in future work.

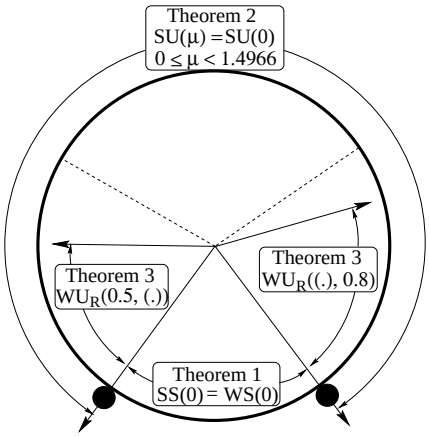

Figure 8: Summary of the stability sets for disk example.

References

[1] A. Bicchi. On the closure properties of robotic grasping. *IJRR*, 14(4):319–334, August 1995.

[2] R. Brost and R.P. Peters. Automatic design of 3d £xtures and assembly pallets. SAND95-2411, Sandia Nat'l Labs, 1997.

[3] R. W. Cottle, J.S. Pang, and R. E. Stone. *The Linear Complementarity Problem*. Academic Press, 1992.

[4] W. S. Howard and V. Kumar. On the stability of grasped objects. *IEEE TRA*, 12(6):904–917, December 1996.

[5] K. Lakshminarayana. Mechanics of form closure. Technical Report 78-DET-32, ASME, 1978.

[6] C. Lanczos. *The Variational Principles of Mechanics*. University of Toronto Press, 1986.

[7] V.-D. Nguyen. The synthesis of force closure grasps in the plane. MS thesis, MIT Dept of ME 1985. AI-TR861.

[8] R. Palmer. *Computational Complexity of Motion and Stability of Polygons*. PhD thesis, Cornell Dept of CS, 1987.

[9] J.S. Pang and J.C. Trinkle. Stability characterizations of rigid body contact problems with coulomb friction. *ZAMM*, 2000, in press.

[10] J.C. Trinkle. On the stability and instantaneous velocity of grasped frictionless objects. *IEEE TRA*, 8(5):560–572, 1992.

[11] J.C. Trinkle. A quantitative test for form closure grasps. In *Proc. IEEE IROS*, pp. 1670–1677, July 1992.

[12] J.C. Trinkle, J.S. Pang, S. Sudarsky, and G. Lo. On dynamic multi-rigid-body contact problems with coulomb friction. TAMU-CS TR 95-003, Texas A&M Dept. of CS, 1995.

[13] J.C. Trinkle, J.S. Pang, S. Sudarsky, and G. Lo. On dynamic multi-rigid-body contact problems with coulomb friction. *ZAMM*, 77(4):267–279, 1997.

[14] J. D. Wolter and J.C. Trinkle. Automatic selection of £xture points for frictionless assemblies. In *Proc. IEEE ICRA*, pp. 528–534, May 1994.